Environmental Earth Sciences (2023) 82:458
https://doi.org/10.1007/s12665-023-11157-x

ORIGINAL ARTICLE

Radiogenic heat production in rocks from the Sabinas Basin (northeastern Mexico) determined by in situ gamma radiation measurements

J. A. Batista-Rodríguez[1] · J. Tolentino-Álvarez[1] · R. Y. Batista-Cruz[1] · Y. Almaguer-Carmenates[1] · F. J. López-Saucedo[1]

Received: 1 November 2022 / Accepted: 29 August 2023 / Published online: 8 September 2023

Abstract

In situ gamma radiation measurements were performed to calculate the radiogenic heat production of sedimentary and igneous rocks from the Sabinas Basin (northeastern Mexico). The sedimentary rocks include Cretaceous shales, sandstones, and limestones. The igneous rocks consist of basalts and granodiorites (Tertiary age). The basalts belong to different volcanic fields (Las Esperanzas, Ocampo, and Las Coloradas), and the granodiorites belong to the Candela-Monclova magmatic belt (Marcelinos, Pánuco, Colorado, and Providencia intrusions). The studied rocks samples yielded values of up to 13.4 ppm, 47.3 ppm, and 9.1% for uranium (U), thorium (Th), and potassium (K), respectively, and their radiogenic heat production (RHP) values ranged from 0.11 to 6.42 μWm^{-3}. The studied rocks were accordingly classified as having low ($<2\ \mu Wm^{-3}$), moderate (2–4 μWm^{-3}), and high ($>4\ \mu Wm^{-3}$) RHP. Most studied rocks were characterized by a low heat production, and only 12% of the measurements indicated samples with moderate and high heat production rates. These latter rocks samples are represented by clastic sedimentary rocks such as shale of the Olmos Formation Maastrichtian age and sandstone of the Pátula Formation Hauterivian–Barremian age, and granodiorites. The highest RHP values in the sedimentary rocks are related to quartz, K-feldspars, and clay contents, and their location of deep faults. The RHP values of granodiorites are associated with their K-feldspar, sphene, zircon, and apatite contents. Such values are different in each of the intrusions and reach the highest magnitudes in the Marcelinos intrusion. The three volcanic fields reported differences in the RHP values, associated with K-feldspar and apatite, and with high and low basement blocks of the Sabinas Basin. The relationship of the RHP values with previously reported heat flow zones indicates the radiogenic contribution of the studied rocks to the heat flow in such basin.

Keywords Gamma-ray spectrometry · Heat-producing · Sabinas Basin · Mexico

Introduction

Radiogenic heat production (RHP) from the decay of uranium (U), thorium (Th), and potassium (K) constitutes one of the most important sources of heat from the Earth's interior (Abbady and Al-Ghamdi 2018). Thus, the determination of the heat produced by the decay U, Th, and K in rocks is a key factor in geothermal exploration (Rybach 1988). The decay of U, Th, and K proceeds from the decay series of ^{238}U, ^{232}Th, and the isotope ^{40}K, respectively. In the rocks, these three radioelements are associated with their mineralogical compositions. Specifically, U has an average abundance of about 3 ppm in the Earth's crust and is a major constituent of some minerals such as uraninite, which is associated with granite-forming minerals. Uranium also appears in common accessory minerals (zircon, apatite, monazite, allanite, and sphene) in igneous and metamorphic rocks (IAEA 2003). Thorium has an average crustal abundance of about 12 ppm. This radioelement appears as a major constituent in minerals such as thorite and uranothorite. It is also found in accessory minerals, for example, monazite, xenotime, zircon, allanite, apatite, sphene, and epidote. Potassium has an average crustal abundance of 2.33 wt%. This radioelement is mainly found in many

✉ J. A. Batista-Rodríguez
josebatista@uadec.edu.mx

[1] Escuela Superior de Ingeniería, Universidad Autónoma de Coahuila, Blvd. Licenciado Adolfo López Mateos S/N, Nueva Rosita, Coahuila, Mexico

rock-forming silicate minerals, such as alkali-feldspars and micas in granitoids (IAEA 2003).

The gamma rays penetrating through geological materials are very useful for measuring the radioelement concentrations within such materials (McCay et al. 2014). The U, Th, and K concentrations can be obtained from samples or through aerial and terrestrial gamma-ray spectrometry measurements. Therefore, these concentrations can be obtained from in situ gamma radiation measurements, that is, taken directly from geological outcrops with handheld gamma-ray detectors (IAEA 2003; McCay et al. 2014; Adagunodo et al. 2019; Akingboye et al. 2021). These in situ measurements can detect gamma rays up to depths of approximately 0.15 m and over diameter of 1 m diameter in outcrops (McCay et al. 2014). According to Rybach (1988) and Aisabokhae and Tampul (2020), outcropping rocks with high concentrations of radioactive elements must have a high heat flow density. This latter, combined with RHP, provides information about the structure and temperature field of the Earth's crust. In turn, the RHP can be inferred from the concentrations of the three radioelements and the density of the rocks considered (Rybach 1988). This is related to the heat produced in the lithosphere, the basement, and the fill of the sedimentary basins (Abbady and Al-Ghamdi 2018). These basin fills mainly consist of sedimentary (clastic and carbonate) and igneous materials, which can produce high RHP rates in sedimentary basins (McCay et al. 2014). Clastic sedimentary rocks generally contain higher U, Th, and K concentrations (IAEA 2003) and, therefore, higher RHP values than carbonate rocks (Hasterok et al. 2018; Cui et al. 2019). Acidic igneous rocks have higher radioactive element concentrations than intermediate and basic rocks (IAEA 2003), which implies an increase in the RHP with an increase in a rock's siliceous content (Cui et al. 2019).

In Mexico, geothermal resources are distributed in marine and continental areas. The former are located mainly in the Gulf of California and the latter in five geothermal fields located in various states across the country. Heat flow studies have confirmed the great potential of geothermal resources in Mexico, with values above 100 mW/m^2 (Prol-Ledesma et al. 2018). Similarly, other studies investigating the depth of magnetic sources and heat flux estimates have revealed values of 85 ± 27 mW/m^2 in the continental zones and 64.7 mW/m^2 in the oceanic zones (Carrillo-de la Cruz et al. 2021).

Over 150 hot spring manifestation sites have been reported in northeastern Mexico, specifically within the Sabinas Basin (Fig. 1; Torres-Rodríguez et al. 1993; Martínez-Estrella et al. 2005; Wolaver et al. 2013; Iglesias et al. 2015; Prol-Ledesma et al. 2018). Such manifestations suggest that this basin could host geothermal deposits. This basin is mainly filled with sedimentary materials (clastic, carbonate, and evaporitic) and igneous rocks (intrusive and extrusive) with basic and intermediate compositions (Eguiluz de Antuñano 2001). The RHP characteristics of each geological unit that comprises this basin should be determined to conduct future geothermal exploration work in the area. Indeed, the RHP will depend on the studied lithologies (Vila et al. 2010). Thereby, this paper presents the results of the calculation of RHP from the U, Th, and K concentrations obtained from the in situ gamma radiation measurements of sedimentary and igneous rock outcrops in the Sabinas Basin.

Geological setting

The Sabinas Basin constitutes a paleogeographic features at the northeastern Mexico, related to the breakup of Pangea during the Late Triassic to Middle Jurassic (Wilson 1990). This geological event allowed the formation of grabens and horsts that controlled the sedimentation patterns in the region during the Mesozoic (Padilla y Sánchez 1986). The Sabinas Basin is the principal graben in the region surrounded by horsts, such as the Coahuila block, the Burro-Peyotes Peninsula, and the Tamaulipas Archipelago. The Coahuila block is composed mainly of Permian sedimentary rocks, with intercalation of volcanic rocks (andesites and dacites). This block is intruded by Permo-Triassic granitic to granodioritic rocks. The Burro-Peyotes Peninsula is composed mainly of metasedimentary rocks. The Tamaulipas Archipelago has a sequence of Middle-Permian Pennsylvanian marine rocks and Triassic intrusive bodies on a Permo-Triassic intrusive basement. The La Mula and Monclova islands are two Permo-Triassic granitic intrusions, that constitute two high basement blocks within this basin (Fig. 1a; Wilson 1990).

The Sabinas Basin is mainly filled with evaporitic, carbonate, and clastic rocks, deposited from the Late Jurassic to the Holocene (Fig. 2). The materials deposited during the Late Jurassic were primarily terrigenous, which generated various geological formations (Eguiluz de Antuñano 2001).

Carbonates and terrigenous rocks were deposited during the Early Cretaceous (Eguiluz de Antuñano 2001). Figures 1b and 2, such as La Mula (Hauterivian–Barremian), Pátula (Hauterivian–Barremian), Cupido (Hauterivian–Aptian), La Peña (Aptian), and Aurora (Albian). Up to 760 m thick shales and clayey limestones were deposited in the La Mula Formation; while sandstone, shale, and conglomerate were deposited in the Pátula Formation (González-Ramos et al. 2008). Moreover, limestone and dolomite with a total thickness of up to 500 m conform the Cupido Formation (Eguiluz de Antuñano 2001). Finally, a 200 m thick sequence of clayey limestones and shales constitutes the La Peña Formation, and micritic limestones of up to 1000 m in thickness correspond to the Aurora Formation (Eguiluz de Antuñano 2001).

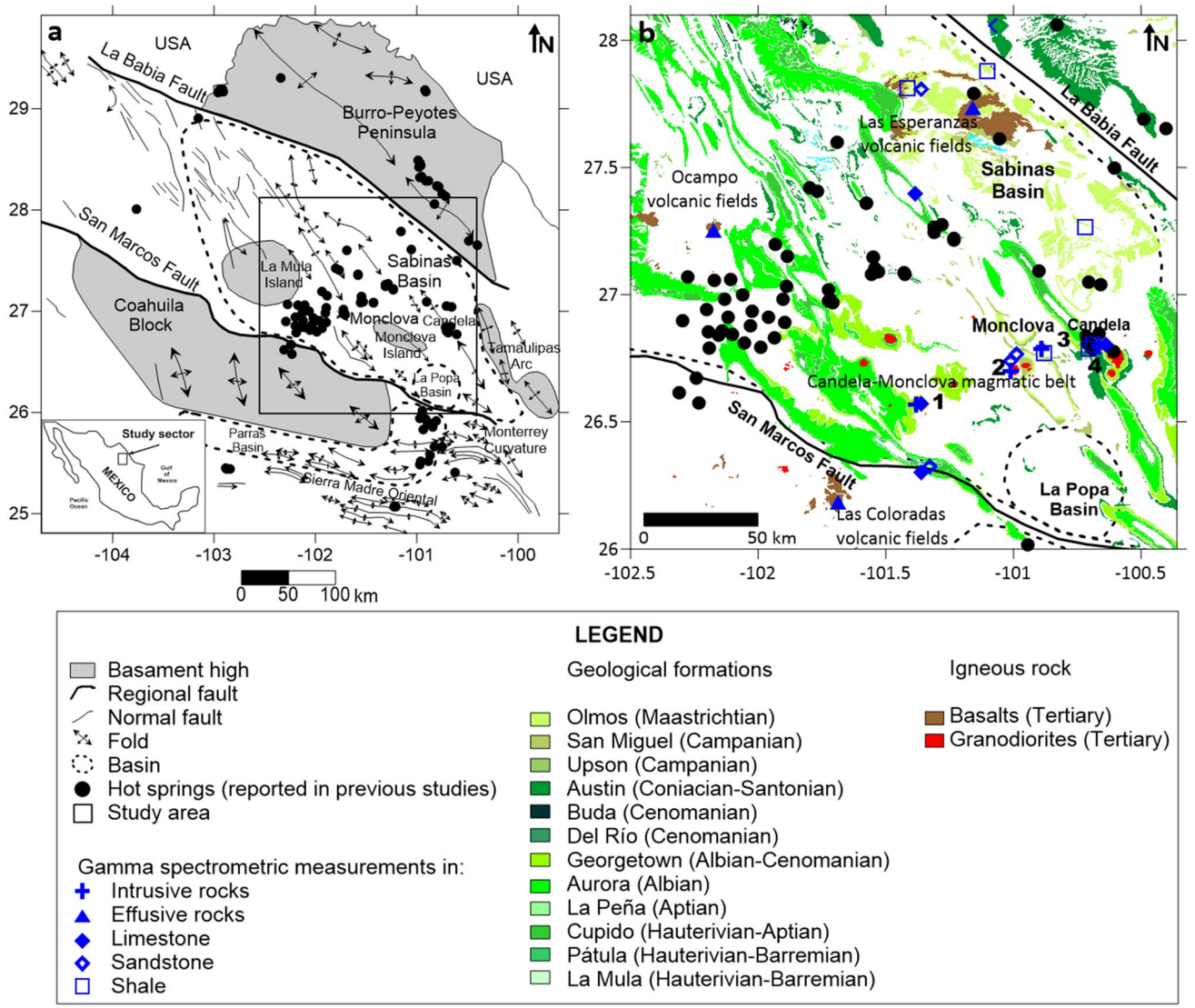

Fig. 1 **a** Structural configuration and tectonic features of northeastern Mexico (modified from Chávez-Cabello et al. 2005). Black rectangle indicates location of the study area. The hot springs were previously reported by Torres-Rodríguez et al. (1993), Martínez-Estrella et al. (2005), Wolaver et al. (2013), Iglesias et al. (2015), Prol-Ledesma et al. (2018), and Tolentino-Álvarez (2022). **b** Geological map of the study area, modified from Barboza-Luna et al. (2008), González-Ramos et al. (2008), Martínez-Rodríguez et al. (2008), Pérez de la Cruz et al. (2008), Romo-Ramírez et al. (2008), and Santiago-Carrasco et al. (2008). 1, 2, 3, and 4 indicate the location of the Marcelinos, Pánuco, Colorado, and Providencia intrusive bodies, respectively

The Late Cretaceous terrigenous and carbonate rocks outcrop in the study area; these include the Georgetown (Albian–Cenomanian), Del Rio (Cenomanian), Buda (Cenomanian), Austin (Coniacian–Santonian), Upson (Campanian), San Miguel (Campanian), and Olmos (Maastrichtian) formations. The Georgetown Formation consists of micritic and argillaceous limestones, with a thickness of up to 300 m (Eguiluz de Antuñano 2001). The Del Río Formation comprises shales and sandstones with a thickness of up to 80 m (Eguiluz de Antuñano 2001). Clayey limestone successions of 23 m and 700 m in thickness make up the Buda and Austin formations, respectively (Eguiluz de Antuñano 2001). The shales of the Upson Formation reach 150 m in thickness (Eguiluz de Antuñano 2001). The San Miguel and the Olmos formations are up to 260 m and 378 m thick, respectively, and both consist of sandstones and shales (Eguiluz de Antuñano 2001).

Various magmatic events originated during the development of the Sabinas Basin, represented principally by different bodies of intrusive and extrusive rocks of Tertiary age that

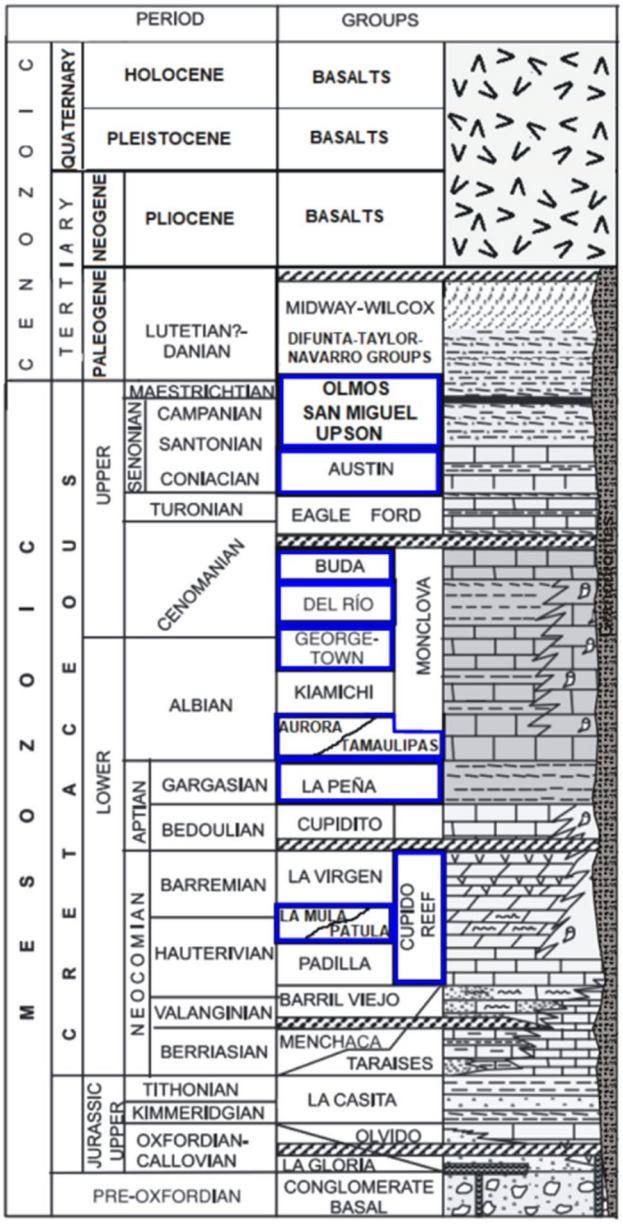

Fig. 2 Stratigraphic column of the Sabinas Basin, modified from Eguiluz de Antuñano (2001). The boxes with a thick blue line show the studied geological formations

outcrop in the region (Eguiluz de Antuñano 2001; Aranda-Gómez et al. 2005). The intrusive igneous rocks affected much of the sedimentary sequence that fills the basin. These igneous rocks are represented by monzonites, monzodiorites, quartz monzonites, granodiorites, and diorites, belonging to the Candela-Monclova magmatic belt (González-Ramos et al. 2008). The extrusive rocks mainly consist of basalts, basanites, and hawaiites, belonging to the Las Esperanzas, Ocampo, and Las Coloradas volcanic fields (Aranda-Gómez et al. 2005).

Table 1 Studied sites and rocks

Latitude (°)	Longitude (°)	Site	Rocks	*N*
26.71	− 101.01	Pánuco	Granodiorite	20
26.80	− 100.89	Colorado	Granodiorite	36
26.58	− 101.38	Marcelinos	Granodiorite	49
27.74	− 101.16	Las Esperanzas	Basalt	227
26.33	− 101.33	La Muralla	Sandstone	138
26.31	− 101.36	La Muralla	Limestone	18
27.82	− 101.36	Rancherías	Sandstone	7
27.41	− 101.39	Obayos	Limestone	129
26.78	− 100.88	Colorado	Shale	4
26.58	− 101.36	Marcelinos	Limestone	51
27.89	− 101.10	Cloete	Shale	13
27.82	− 101.41	Rancherías	Shale	16
27.28	− 100.72	San Patricio	Shale	12
28.07	− 101.07	Autopista	Limestone	32
26.78	− 100.88	Colorado	Shale	5
26.81	− 100.69	Candela	Shale	13
26.80	− 100.67	Candela	Granodiorite	6
26.78	− 100.99	Candela	Sandstone	6
26.81	− 100.64	Candela	Limestone	21
26.80	− 100.70	Candela	Shale	6
26.75	− 101.01	Colorado	Sandstone	9
26.19	− 101.69	Las Coloradas	Basalt	100
27.26	− 102.17	Ocampo	Basalt	61

N: number of measurements

Materials and methods

The calculation of RHP was carried out using 970 in situ gamma-ray spectrometry measurements obtained at 23 sites in the Sabinas Basin (Fig. 1b; Table 1). Of these sites, 499 measurements were made at seven igneous rock sites, of which four represented intrusive rocks (granodiorites of the Marcelinos, Pánuco, Colorado, and Providencia intrusive bodies; 111 measurements), and three comprised extrusive rocks (basalts; 388 measurements). A total of 471 measurements were also performed at 16 sedimentary rock sites. Of these sites, four consisted of sandstone (160 measurements), six were represented by limestone (251 measurements), and six were composed of shale (60 measurements). The granodiorite (Tertiary) sites were located at the Candela-Monclova magmatic belt, and the basalt (Tertiary) sites in the Las Esperanzas, Ocampo, and Las Coloradas volcanic fields (Fig. 1b). The sites hosting the sedimentary rocks were characterized by clastic rocks (shale and sandstone) and carbonates (limestone). These rocks belong to different Early Cretaceous (Figs. 1b, 2; La Mula, Pátula, Cupido, La Peña, and Aurora) and Late Cretaceous (Georgetown, Del Río, Buda, Austin, Upson, San Miguel, and Olmos) geological formations.

Gamma spectrometric measurements were performed using a portable NaI(Tl) γ-ray spectrometer (spectrometer RS-125) manufactured by Radiation Solution Inc. The measurements were obtained directly from the surface of each rock's outcrop as far as possible from fractures and voids in the rocks, with a counting time of 120 s (IAEA 2003). This sampling period is used normally in most conditions because gives good quality data (Radiation Solution Inc. 2015). The device had a self-stabilizer to correct for surrounding background radiation. This allowed data to be obtained without the influence of changes in temperature or significant changes in gamma-ray emission. This equipment had been factory-calibrated using test pads, did not need radioactive sources for proper operation, and had a high sensitivity using a large 2.0 × 2.0 NaI crystal of 103 cm^3 in size to detect concentrations of U (ppm), Th (ppm), and K (%) (Radiation Solution Inc. 2015). The equilibrium conditions of the ^{238}U and ^{232}Th decay series were considered, and therefore, the term "equivalent" and its abbreviation "e" are used (i.e., eU and eTh) to refer to the U and Th concentrations estimated from these series.

Rock samples were obtained from each studied site and their density was measured using the hydrostatic immersion method classic; these average density values were used to calculate the RHP (Table 2). For the granodiorite samples, a density of 2.74 g cm^{-3} was used. A density of 2.65 g cm^{-3} was used for the basalts; 2.61 g cm^{-3} for the sandstones; 2.64 g cm^{-3} and at some sites 2.6 g cm^{-3} (Colorado and Candela) for the shales; and 2.60 g cm^{-3} and at some sites 2.64 g cm^{-3} (Autopista) for the limestones. The RHP (μWm^{-3}) produced by radioactivity in the Sabinas Basin rocks was computed using the following equation (Rybach 1988):

$$\mathrm{RHP} = \rho\left(9.52C_{\mathrm{U}} + 2.56C_{\mathrm{Th}} + 3.48C_{\mathrm{K}}\right)10^{-5}, \quad (1)$$

where ρ is the bulk density of the rock; C_U and C_{Th} are the U and Th concentrations in weight ppm; C_K is the K

Table 2 Rock densities of the study sites (g cm^{-3})

Site	Rocks	N1	N2	N3	N4	N5	N6	N7	N8	Average
Pánuco	Granodiorite	2.734	2.737	2.736	2.731	–	–	–	–	2.735
Colorado	Granodiorite	2.748	2.745	2.741	2.737	–	–	–	–	2.743
Marcelinos	Granodiorite	2.742	2.740	2.732	2.739	–	–	–	–	2.738
Las Esperanzas	Basalt	2.652	2.653	2.654	2.651	2.656	2.655	2.656	2.650	2.653
La Muralla	Sandstone	2.615	2.605	2.618	2.612	2.610	2.620	2.617	2.611	2.614
La Muralla	Limestone	2.608	2.609	2.614	2.611	–	–	–	–	2.611
Rancherías	Sandstone	2.620	2.623	2.619	–	–	–	–	–	2.621
Obayos	Limestone	2.608	2.605	2.599	2.609	2.597	2.604	2.602	–	2.603
Colorado	Shale	2.599	2.596	–	–	–	–	–	–	2.598
Marcelinos	Limestone	2.596	2.604	2.601	–	–	–	–	–	2.60
Cloete	Shale	2.644	2.643	2.641	–	–	–	–	–	2.643
Rancherías	Shale	2.639	2.635	2.638	–	–	–	–	–	2.637
San Patricio	Shale	2.640	2.643	2.639	–	–	–	–	–	2.641
Autopista	Limestone	2.642	2.640	2.637	2.639	–	–	–	–	2.64
Colorado	Shale	2.602	2.607	–	–	–	–	–	–	2.605
Candela	Shale	2.60	2.604	2.601	–	–	–	–	–	2.602
Candela	Granodiorite	2.746	2.748	–	–	–	–	–	–	2.747
Candela	Sandstone	2.617	2.613	–	–	–	–	–	–	2.615
Candela	Limestone	2.60	2.596	2.595	–	–	–	–	–	2.597
Candela	Shale	2.598	2.60	–	–	–	–	–	–	2.599
Colorado	Sandstone	2.611	2.606	–	–	–	–	–	–	2.609
Las Coloradas	Basalt	2.648	2.654	2.652	2.652	2.651	–	–	–	2.651
Ocampo	Basalt	2.651	2.654	2.655	2.657	–	–	–	–	2.654

N1–N8 indicate the measured samples

Average densities used

Granodiorite: 2.74 g cm^{-3}

Basalt: 2.65 g cm^{-3}

Sandstone: 2.61 g cm^{-3}

Limestone: 2.61 g cm^{-3} (all sites use 2.60 g cm^{-3}, except the Autopista with 2.64 g cm^{-3})

Shale: 2.62 g cm^{-3} (Colorado and Candela: 2.60 g cm^{-3}; Cloete, Rancherías and San Patricio: 2.64 g cm^{-3})

concentration in weight %. These concentrations were multiplied by the heat generation constants (the amount of heat released per gram of U, Th, and K per unit time). Statistical parameters such as the minimum, maximum, and average values, and standard deviation of the radioelements and RHP in each studied rock type of the Sabinas Basin were computed. Rocks with RHP values greater than 4 μWm^{-3} were considered as having a high RHP potential (McCay et al. 2014). Similarly, rocks with RHP values of less than 2 μWm^{-3} were considered as having a low RHP rate while rocks with RHP values between 2 and 4 μWm^{-3} exhibited moderate RHP.

Results

In all the studied rocks, the obtained concentrations of eU ranged from 0 to 13.4 ppm with an average of 2.02 ppm, the concentrations of eTh varied from 0 to 47.3 ppm with an average of 6.86 ppm, and the range of K concentrations ranged from 0 to 9.1% with an average of 1.55%. According to the concentrations of these radioelements, RHP values from 0.11 to 6.42 μWm^{-3} (average of 1.11 μWm^{-3}) were obtained (Table 3). Most RHP values (85.15%) were less than 2 μWm^{-3} (Fig. 3), while 13.5% of the values ranged from 2 to 4 μWm^{-3}, and only 1.35% exceeded 4 μWm^{-3}. These results indicate that most of the studied rocks were considered to have a low heat production potential. Only 1.35% of the measurements (13 measurements out of a total of 970) yielded high RHP values (McCay et al. 2014). Later, the radioactive characteristics and the RHP of each geological formation and lithologies studied will be described.

Figure 4 shows that all three radioelements correlated very well with the RHP; the higher the concentrations of the three radioelements, the higher the RHP. Of these three radioelements, the eU was the one that contributed the most to the RHP (48.1%), followed by the eTh (40.6%; Table 4).

Radioelement contents and heat production in sedimentary rocks

The highest concentrations of eU, eTh, and K, as well as the highest values of RHP, were obtained from sedimentary rocks, (Tables 3, 4); therefore, sedimentary rocks were found to produce the highest amounts of radiogenic heat in the Sabinas Basin. These rocks were characterized by eU concentrations ranging from 0.01 to 13.4 ppm with an average of 2.39 ppm; their eTh concentrations varied from 0 to 47.3 ppm with an average of 7.79 ppm, and K concentrations from 0 to 9.1% with an average of 1.73%. In addition, these rocks yielded RHP values ranging from 0.11 to 6.42 μWm^{-3} with an average of 1.27 μWm^{-3}. These values were higher than those obtained from sedimentary rocks from the Gulf of Mexico (0.4–1.5 μWm^{-3}; Nagihara et al. 1996; Netto 2017) and other regions of the world, for example, values from 1 μWm^{-3} in a compilation study worldwide (Vila et al. 2010) and 0.97 μWm^{-3} in Sichuan Basin, China (Zhu et al. 2018).

Most of the RHP values obtained from the sedimentary rocks of the Sabinas Basin (75.58%, 356 measurements out of a total of 471) were less than 2 μWm^{-3} (Fig. 5a). These values indicate that most sedimentary rocks had a low RHP potential. Out of the measurements, 22.51% (106 measurements) had RHP values between 2 and 4 μWm^{-3}, characterizing rocks with a moderate RHP potential. Less than 2% of the values (nine measurements) exceeded 4 μWm^{-3}. These latter values (2–4 μWm^{-3} and greater than 4 μWm^{-3}) were recorded in clastic rocks (Fig. 5b), mainly shales of the Olmos Formation and sandstones of the Pátula Formation (Table 3; Fig. 6); these were considered as producing high amounts of heat (McCay et al. 2014; Adagunodo et al. 2019).

In the sedimentary rocks, the RHP values correlate very well with the three radioelements (Fig. 6), mainly with eTh and eU, Fig. 6 shows that the carbonate rocks fit better than clastic rocks with the general correlation of the three radioelements with RHP. This fit must be related to the lower radioactive heterogeneity of the carbonate rocks according to the SD values (Table 3). Therefore, this correlation indicates a greater linear dependence of the heat production with the concentrations of the radioelements in the carbonate rocks. For the clastic rocks, the Olmos Formation shales fit better with the general correlation and showed the highest eTh, eU, and RHP values (Fig. 6a, b). The Pátula Formation (sandstones) exhibited a similar behavior but with a lower fit and lower eTh, eU, and RHP values (Fig. 6a, b). The analysis of the correlation between the RHP and K indicates that the Olmos Formation shales did not fit the general correlation of the sedimentary rocks, although these were associated with the highest RHP values (Fig. 6c). In the sedimentary rocks, eU was the radioelement that most contributed to the RHP (56.8%), followed by eTh (34.6%), and K (8.6%; Table 4). These contributions are like those reported by Cui et al. (2019) in Meso-Cenozoic sedimentary rocks of the Bohai Bay basin, China.

Among the sedimentary rocks, the clastic rocks had the highest radioactive element concentrations and highest RHP (Table 3; eU, from 0.01 to 13.4 ppm, and an average of 3.23 ppm; eTh, from 0.4 to 47.3 ppm, and an average of 14.6 ppm; K, from 0.1 to 91%, and an average of 9.45%; RHP, from 0.21 to 6.42 μWm^{-3}, and an average of 2.1 μWm^{-3}). Most of these rocks exhibited low-moderate RHP values, because 49.10% (108 measurements out of a total of 220) of the RHP values were less than 2 μWm^{-3}, and 46.82% (103 measurements) ranged between 2 and 4 μWm^{-3}. Some clastic rocks exhibited a high RHP potential;

Table 3 Statistical parameters (SP) of the gamma-ray spectrometric data and radioactive heat production (RHP) of the Sabinas Basin rocks

Rock unit	SP	eU ppm	eTh ppm	K %	RHP μWm^{-3}	Geological formation	SP	eU ppm	eTh ppm	K %	RHP μWm^{-3}
All rocks (970)	Min	0	0	0	0.11	La Peña formation (45)	Min	0.01	0	0	0.14
	Max	13.4	47.3	9.1	6.42		Max	3.1	3.4	0.3	0.80
	A	2.02	6.86	1.55	1.11		A	1.52	1.26	0.08	0.47
	SD	1.61	6.5	1.78	0.87		SD	0.78	0.65	0.08	0.17
Granodiorite (111)	Min	0.4	3.7	1.1	0.57	Aurora formation (11)	Min	0.1	1.0	0	0.09
	Max	9.1	30.2	6.0	4.57		Max	3.3	3.4	0.3	0.99
	A	3.11	9.83	2.69	1.76		A	0.98	1.98	0.14	0.39
	SD	1.70	5.53	1.20	0.87		SD	0.96	0.68	0.1	0.27
Basalt (388)	Min	0	0.9	0.3	0.19	Georgetown formation (16)	Min	0.4	1.3	0	0.21
	Max	4.4	10.7	2.9	1.60		Max	6.9	16.5	3.3	3.10
	A	1.26	4.88	1.0	0.74		A	2.40	6.21	1.45	1.14
	SD	0.88	1.88	0.38	0.31		SD	1.73	4.83	1.18	0.82
Limestone (251)	Min	0.01	0	0	0.11	Del Río formation (6)	Min	0.6	1.4	0.2	0.33
	Max	6.9	16.5	3.3	3.10		Max	2.1	4.2	0.5	0.58
	A	1.66	1.82	0.22	0.55		A	1.31	3.1	0.36	0.43
	SD	0.94	1.90	0.47	0.33		SD	0.54	1.0	0.1	0.08
Shale (69)	Min	0.4	1.4	0.2	0.43	Buda formation (62)	Min	0.01	0	0	0.11
	Max	13.4	44.1	2.8	6.42		Max	3.5	3.8	1.1	0.87
	A	4.54	13.4	1.49	2.17		A	1.61	1.29	0.09	0.49
	SD	2.77	9.2	0.68	1.24		SD	0.78	0.79	0.21	0.17
Sandstone (160)	Min	0.01	0.4	0.1	0.21	Austin formation (42)	Min	0.2	0.1	0	0.24
	Max	7.7	47.3	9.1	4.73		Max	4.5	6.8	1.1	1.47
	A	2.74	15.0	4.19	2.06		A	2.16	1.95	0.27	0.69
	SD	1.55	7.16	2.45	0.83		SD	0.85	1.58	0.29	0.27
La Mula formation (45)	Min	0.01	0.3	0	0.15	Upson formation (12)	Min	0.4	3.1	2.0	0.82
	Max	4.0	4.2	0.4	1.14		Max	5.5	14.5	2.8	1.61
	A	1.38	1.85	0.19	0.48		A	3.25	10.3	2.32	1.30
	SD	0.80	0.77	0.11	0.18		SD	1.52	3.14	0.21	0.27
Pátula formation (138)	Min	0.01	4.1	1.0	0.72	San Miguel formation (15)	Min	0.6	0.4	0.1	0.21
	Max	7.7	47.3	9.1	4.73		Max	5.2	5.1	0.7	1.44
	A	2.74	16.5	4.75	2.21		A	2.48	2.58	0.41	0.82
	SD	1.58	6.31	2.17	0.77		SD	1.30	1.20	0.18	0.34
Cupido formation (30)	Min	0.01	0.1	0	0.17	Olmos formation (49)	Min	0.9	7.0	0.5	1.0
	Max	3.4	2.5	0.5	0.84		Max	13.4	44.1	2.4	6.42
	A	1.44	1.16	0.06	0.44		A	5.06	15.4	1.41	2.44
	SD	0.76	0.62	0.11	0.18		SD	2.73	9.13	0.50	1.20

Min., Max, A, and SD: minimum, maximum, average, and standard deviations, respectively. The number of measurements is shown in parentheses

indeed, a little more than 4% (nine measurements) of the RHP values exceeded 4 μWm^{-3} (Fig. 5).

Shales were the clastic rocks of the study region with the highest eU concentrations (from 0.4 to 13.4 ppm, and an average of 4.54 ppm; Table 3) and the highest RHP values (from 0.43 to 6.42 μWm^{-3}, and an average of 2.17 μWm^{-3}). These values indicate that the shales produced the most heat in the Sabinas Basin. The sandstones showed the highest eTh concentrations (from 0.4 to 47.3 ppm, with an average of 15.0 ppm) and K (from 0.1 to 9.1%, and an average of 4.19%), with RHP values ranging from 0.21 to 4.73 μWm^{-3} (average of 2.06 μWm^{-3}).

Among the sedimentary rocks, the clastic rocks showed a higher RHP potential from eTh and K than carbonate rocks, which are in agreement with the results obtained from previous research in other countries, for example, China (Cui et al. 2019). Particularly in shales, the eU contributed 51.1% of RHP, followed by the eTh (41.0%), while in sandstones,

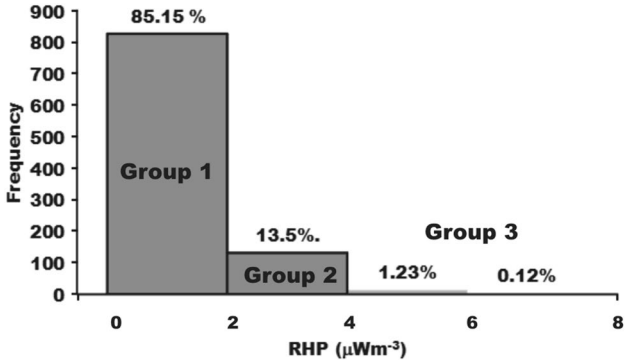

Fig. 3 Histogram showing the distribution of the radiogenic heat production (RHP, μWm^{-3}) of all studied rock samples from the Sabinas Basin. The percentage of total measurements is indicated above the vertical bars. Group 1: RHP < 2 μWm^{-3}), low RHP; group 2: RHP between 2 and 4 μWm^{-3}, moderate RHP; group 3: RHP > 4 μWm^{-3}, high RHP

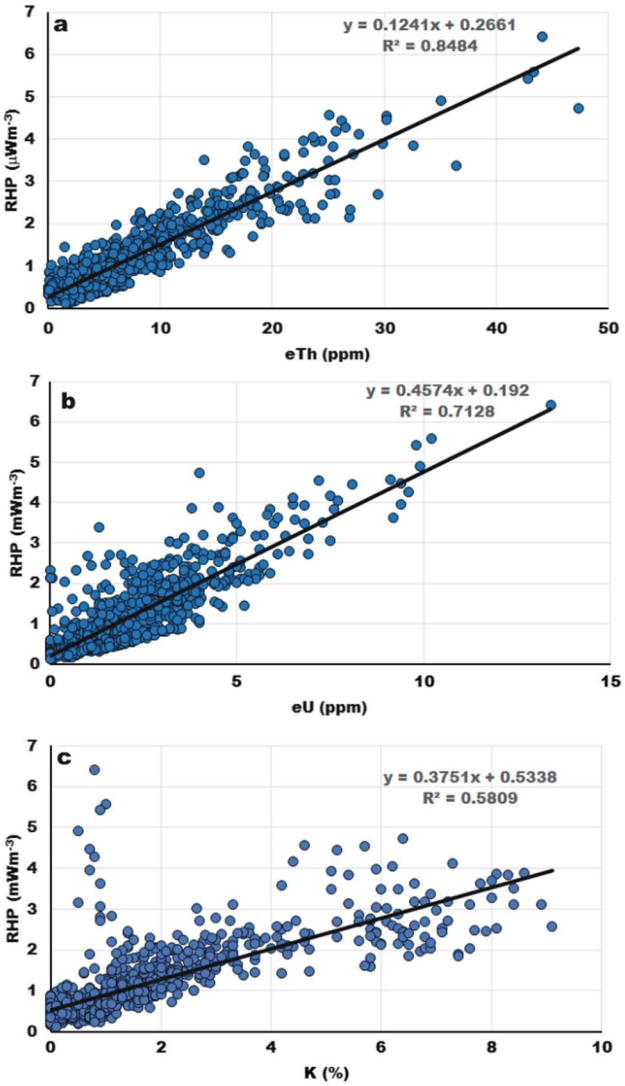

Fig. 4 Relationship between the radiogenic heat production (RHP) and the activity concentration of radioelements in all studied rock samples from the Sabinas Basin. **a** RHP and eTh; **b** RHP and eU; **c** RHP and K

the eTh contributed 48.1% and the eU, 34.5%. The highest eU concentrations in the shales were recorded in the Olmos Formation (Tables 2 and 3), with values ranging from 0.9 to 13.4 ppm, and an average of 5.06 ppm. The sandstone rocks with the highest eTh and K concentrations and high RHP values belong to the Pátula Formation (Tables 2, 3). The sandstone rocks from the Olmos Formation also yielded high eTh concentrations.

Higher RHP values were reported in the sedimentary rocks of the Sabinas Basin than in other regions worldwide, particularly in the shales and sandstones. For example, in a compilation study worldwide (Vila et al. 2010) and in Sichuan Basin, China (Zhu et al. 2018), average RHP values from shales of 1.7 and 1.07 μWm^{-3}, respectively, are reported. Hasterok et al. (2018), in another compilation study worldwide, also reported values of 2.9 μWm^{-3} for aluminous shales and 1.7 μWm^{-3} for iron shales. In our study area, the average RHP value (2.17 μWm^{-3}) in the shale was greater than most of the average values obtained by the abovementioned authors. This difference likely suggests the presence of aluminous and iron shales in this basin (Hasterok et al. 2018). In the sandstones, Vila et al. (2010) and Zhu et al. (2018) reported average RHP values of 0.90 and 0.83 μWm^{-3}, respectively. Hasterok et al. (2018) also reported average RHP values ranging from 0.31 to 2.2 μWm^{-3} in different types of sandstone. In the sandstones of the Sabinas Basin, the average RHP value (2.06 μWm^{-3}) was twice as high as most of the values reported in the aforementioned literature.

Within the sedimentary rocks of the Sabinas Basin, the carbonate rocks (limestone) were characterized by having the lowest eU, eTh, and K concentrations, as well as the lowest RHP values. Therefore, the limestones of the studied basin were the rocks with the lowest RHP potential. Most of these rocks were characterized by a low heat production because 98.80% of the RHP values (248 measurements out of a total of 251) were less than 2 μWm^{-3} (Figs. 5c, 6). Only three measurements (1.20% of the total) ranged between 2 and 4 μWm^{-3}, representing rocks with a high RHP potential. In limestones, the RHP was mainly correlated with the eU (0.87), followed by K (0.77) and eTh (0.74), indicating that increases in these three radioelements could generate increases in RHP. Of these three radioelements, the eU was the one that contributed the most to the RHP with 72.3.8%, followed by the eTh with 24.2% (Table 4).

The comparison of the RHP values of the limestones from the Sabinas Basin with limestones from other regions of the world (Vila et al. 2010; Hasterok et al. 2018; Zhu et al. 2018)

Table 4 Average concentrations of radioelements and radiogenic heat production (RHP) in rocks from the Sabinas Basin

Rock unit/geological formation	eU	eTh	K	Heat production rate due to				Contribution (%) due to		
	ppm	ppm	%	eU	eTh	K	Total	eU	eTh	K
All rocks (970)	2.02	6.86	1.55	0.50	0.46	0.14	1.11	48.1	40.6	11.3
Intrusive (111)	3.11	9.83	2.69	0.81	0.69	0.26	1.76	45.3	39.4	15.3
extrusive (549)	1.26	4.88	1.0	0.32	0.33	0.1	0.74	38.0	48.0	14.0
Limestone (251)	1.66	1.82	0.22	0.41	0.12	0.02	0.55	72.3	24.5	3.2
Shale (60)	4.54	13.4	1.49	1.14	0.90	0.13	2.17	51.1	41.0	7.9
Sandstone (160)	2.74	15.0	4.19	0.68	1.0	0.38	2.06	34.5	48.1	17.4
La Mula formation (45)	1.38	1.85	0.19	0.34	0.12	0.02	0.48	66.3	29.7	4.0
Pátula formation (138)	2.74	16.5	4.75	0.68	1.10	0.43	2.21	30.0	50.7	19.3
Cupido formation (30)	1.44	1.16	0.06	0.36	0.07	0.01	0.44	76.9	21.9	1.2
La Peña formation (45)	1.52	1.26	0.08	0.38	0.08	0.01	0.47	74.8	23.0	2.2
Aurora formation (11)	0.98	1.98	0.14	0.25	0.13	0.01	0.39	53.4	42.5	4.10
Georgetown formation (16)	2.40	6.21	1.45	0.60	0.41	0.13	1.14	53.5	36.6	9.9
Del Río formation (6)	1.31	3.1	0.36	0.25	0.16	0.02	0.43	56.1	37.9	6.0
Buda formation (62)	1.61	1.29	0.09	0.40	0.08	0.01	0.49	76.5	21.5	2.0
Austin formation (42)	2.16	1.95	0.27	0.53	0.13	0.03	0.69	77.5	19.0	3.5
Upson formation (12)	3.25	10.3	2.32	0.62	0.53	0.16	1.31	45.5	41.5	13.0
San Miguel formation (15)	2.48	2.58	0.41	0.61	0.17	0.04	0.82	72.2	23.1	4.7
Olmos formation (49)	5.06	15.4	1.41	1.27	1.04	0.13	2.44	52.0	41.6	6.4

The number of measurements is indicated in parentheses

shows that the former had higher or relatively similar RHP values (Table 4). Indeed, Vila et al. (2010), Hasterok et al. (2018), and Zhu et al. (2018) reported average RHP values of 0.47, 0.56, and 0.40 μWm^{-3}, respectively, for limestones from other regions worldwide.

Radioelement contents and heat production in igneous rocks

The igneous rocks comprise the second most significant rock group contributing to the RHP at the Sabinas Basin (Table 3). These rocks had eU concentrations ranging between 0 and 9.1 ppm, with an average of 1.67 ppm. In addition, they yielded eTh concentrations between 0.9 and 30.2 ppm, with an average of 5.98 ppm, and K concentrations between 0.3 and 6.0 ppm, with an average of 1.38. The RHP values of these rocks ranged between 0.19 and 4.57 μWm^{-3} with an average of 0.97 μWm^{-3}. The highest values of the three radioelements and the RHP were obtained from the intrusive igneous rocks (granodiorites). In these rocks, the average values of U, Th, K, and RHP were 3.11 ppm, 9.83 ppm, 2.69%, and 1.76 μWm^{-3}, respectively. This average RHP value was greater than 0.99 μWm^{-3}, which was reported by Carrillo-de la Cruz et al. (2020) as the highest average value recorded in the Sabinas Basin and associated with the youngest intrusive igneous rocks. In extrusive igneous rocks (basalts), up to 4.4 ppm, 10.7 ppm, and 2.9% concentrations of eU, eTh, and K, respectively, and a maximum of 1.60 μWm^{-3} of RHP, were reported (Table 3).

Most igneous rocks were characterized by a low RHP, and 94.18% of the RHP values (470 measurements) were less than 2 μWm^{-3} (Fig. 7). Only 5.01% of the RHP values (25 measurements) were between 2 and 4 μWm^{-3}, and 0.81% (four measurements) exceeded 4 μWm^{-3}; this indicates that some these rocks were associated with moderate and high RHP potentials. These rocks mainly consisted of the granodiorites from the Marcelinos intrusion (Fig. 8). In the granodiorites, 73.87% of the RHP values were less than 2 μWm^{-3}, 22.53% varied between 2 and 4 μWm^{-3}, and 3.60% (only four measurements) exceeded 4 μWm^{-3}. Such values indicate that only some rocks (i.e., the granodiorites from the Marcelinos intrusion) were characterized by a high RHP potential (McCay et al. 2014). Generally, most of the studied granodiorites from all intrusions exhibited low–moderate heat production. In turn, all of the studied basalts revealed a low RHP potential, because 100% of the RHP values were less than 2 μWm^{-3}.

In general, the RHP values of the igneous rocks correlated very well with the three radioelements (Fig. 8). Figure 8 shows that the extrusive rocks (basalts) had lower concentrations of the three radioelements and lower values of RHP (less than 2 μWm^{-3}) than their intrusive counterparts (granodiorites). Indeed, the granodiorites showed higher RHP values from eU and eTh than the basalts (eU, 45.3%, and eTh, 39.4% in granodiorite; eTh, 48%, and eU, 38% in

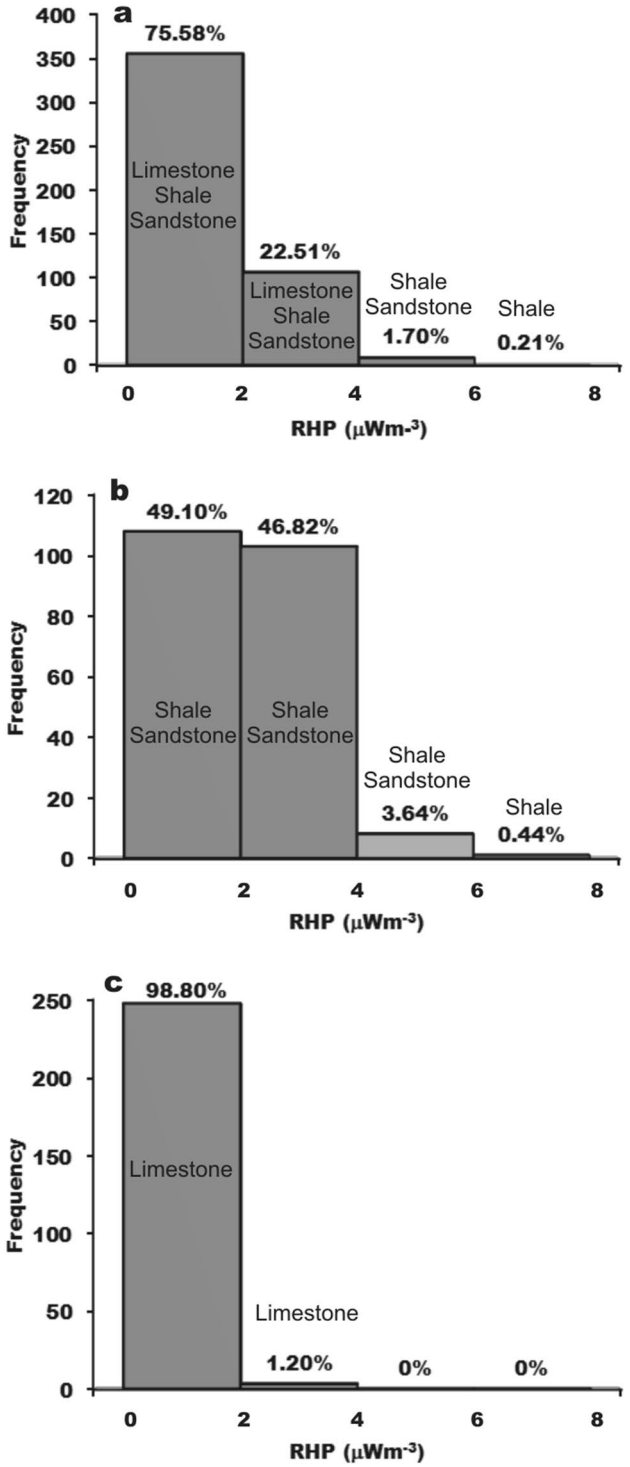

Fig. 5 Histogram showing the distribution of the radiogenic heat production (RHP, μWm^{-3}) of sedimentary rocks from the Sabinas Basin. **a** All types of sedimentary rocks; **b** clastic rocks; c) carbonate rocks. The percentage of total measurements is indicated above the vertical bars. The horizontal axis indicates the RHP ranges (0–2, 2–4, 4–6, and 6–8 $\mu Wm.^{-3}$

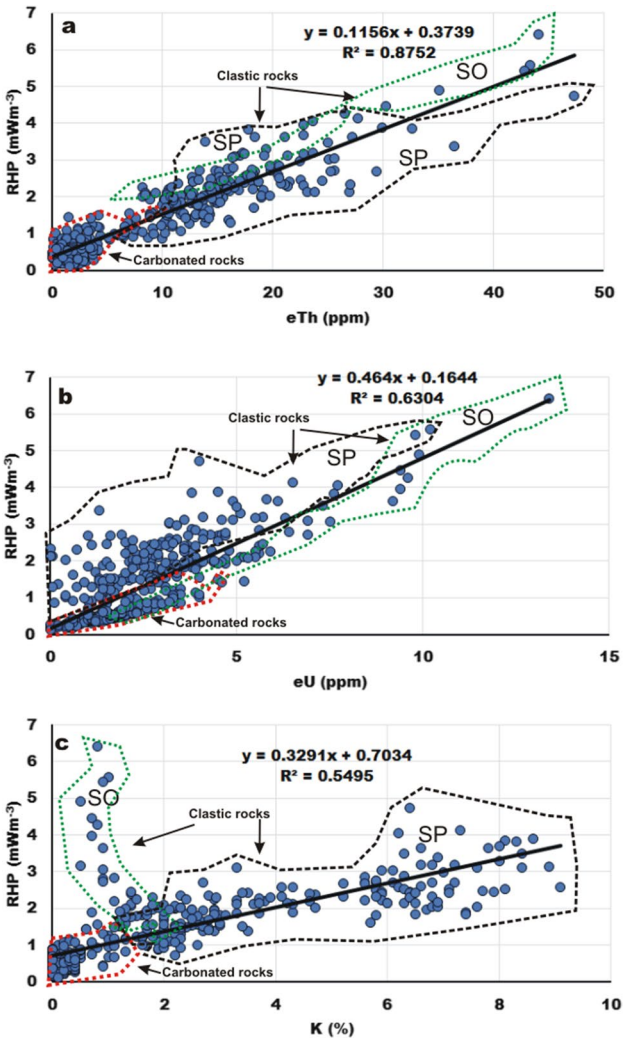

Fig. 6 The relation between the radiogenic heat production (RHP) and the activity concentration of radioelements in the sedimentary rocks from the Sabinas Basin. **a** RHP and eTh; **b** RHP and eU; **c** RHP and K. *SO* shale of the Olmos formation, *SP* sandstone of the Pátula formation. The dotted red, green, and black line indicate the limits of the carbonated rocks, shales, and sandstones, respectively

basalts; Table 4). The basalts experienced the highest heat production from Th (48%).

In the extrusive rocks, the basalts of the Las Coloradas volcanic field yielded the highest radioactive element concentrations and RHP values, followed by the Ocampo and Las Esperanzas fields (Fig. 8).. The zone characterized by intrusive rocks in Fig. 8 mainly consists of rocks belonging to the Marcelinos intrusion, which are characterized by the highest values of the three radioelements and the RHP (greater than 2 μWm^{-3}). The mixed zone of extrusive and intrusive rocks (Fig. 8) is occupied by the Pánuco,

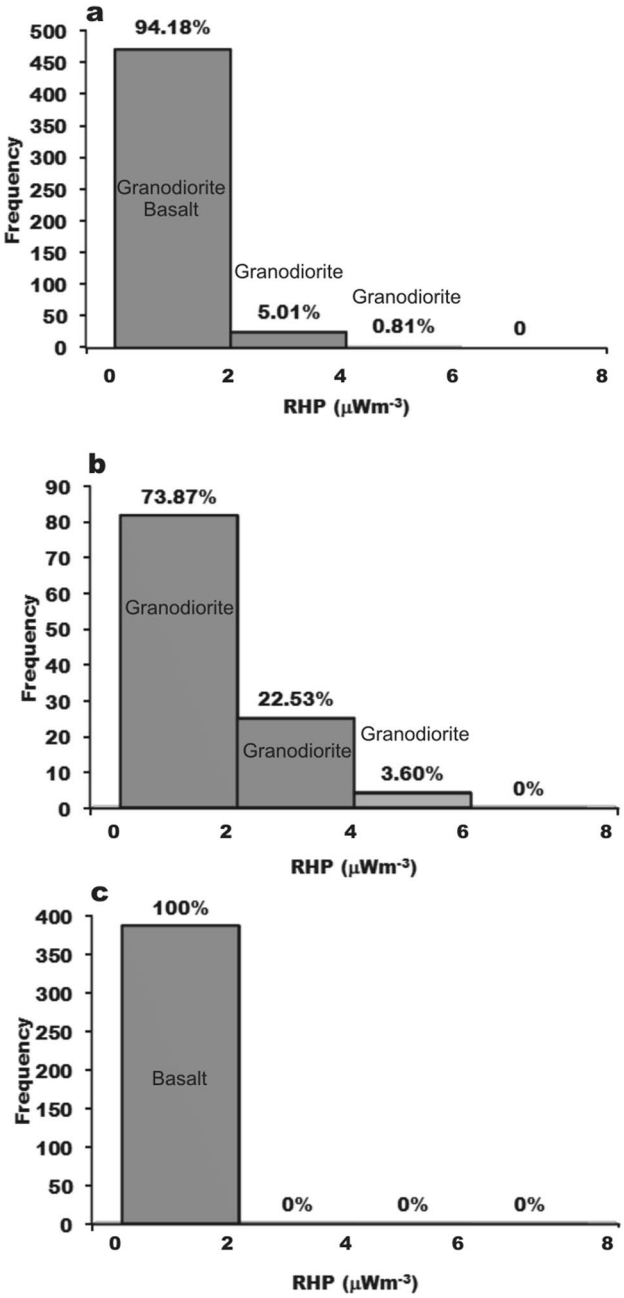

Fig. 7 Histogram showing the distribution of the radiogenic heat production (RHP, μWm^{-3}) of the igneous rocks from the Sabinas Basin. **a** All types of igneous rocks; **b** intrusive rocks (granodiorite); **c** extrusive rocks (basalt). The percentage of total measurements is indicated above the vertical bars. The horizontal axis indicates the RHP ranges (0–2, 2–4, 4–6, and 6–8 $\mu Wm.^{-3}$

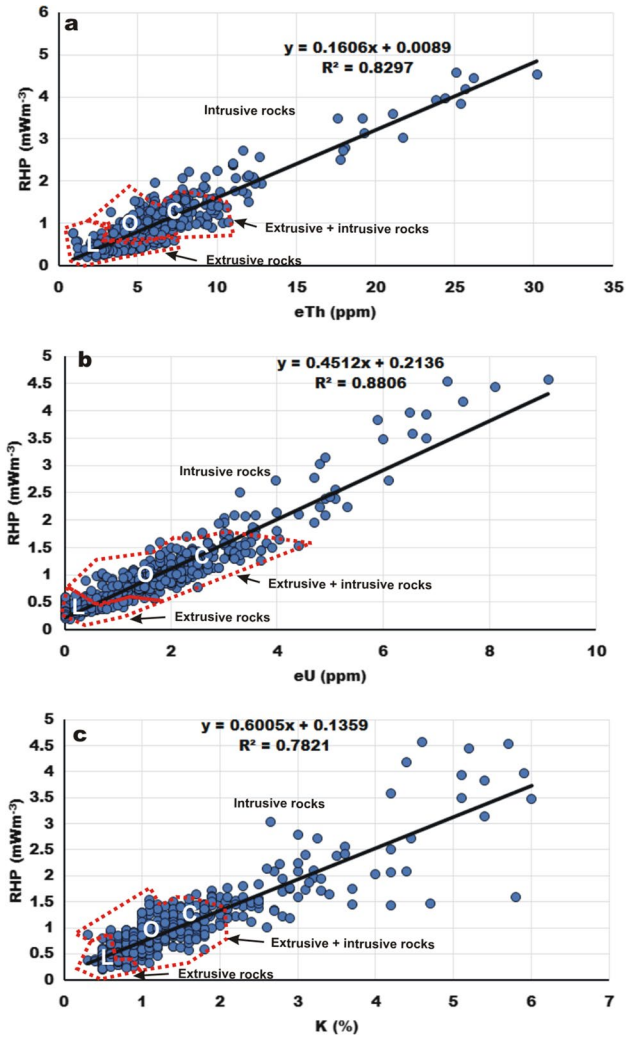

Fig. 8 The relation between the radiogenic heat production (RHP) and the activity concentration of radioelements in the igneous rocks from the Sabinas Basin. **a** RHP and eTh; **b** RHP and eU; **c** RHP and K. L, O, and C denote the Las Esperanzas, Ocampo, and Las Coloradas volcanic fields, respectively. The dotted red line indicates the boundary of the extrusive igneous rocks and the zone where are mixture of extrusive and intrusive rocks

Providencia, and Colorado intrusions, of which Pánuco revealed the highest radioactive element concentrations and RHP values, while Colorado had the lowest values.

The average RHP value (1.76 μWm^{-3}) of the granodiorites in the Sabinas Basin was lower than that reported in some regions of the world (e.g., 2.07 μWm^{-3} in Vila et al. 2010) and higher than that of others (e.g., 1.5 μWm^{-3} in Hasterok et al. 2018 and 1.404 μWm^{-3} in Aisabokhae and Tampul 2020). In turn, the average RHP value of the basalts in this basin (0.74 μWm^{-3}) was higher than that reported by Hasterok et al. (2018) (0.54 μWm^{-3}) in other regions of the world. Similarly, the average RHP value of the basalts from this basin was higher than the averages of alkalic, calc-alkaline, and tholeiitic basalts (0.7, 0.3, and 0.05, respectively) reported by Vila et al. (2010). This result must be related to the alkaline character of the basalts of the Sabinas Basin (Valdez-Moreno 2001; Aranda-Gómez et al. 2005; Valdez-Moreno et al. 2011).

Discussion

Clastic sedimentary rocks specifically shales, and sandstones, are the ones that produce the most radiogenic heat in the Sabinas Basin (Table 3). Its RHP values are higher than those reported in the Gulf of Mexico and other sites, which indicates its high contribution to the relatively high heat flow reported in northeastern Mexico (60–80 mWm^{-2}; Prol-Ledesma et al. 2018; Prol-Ledesma and Morán-Zenteno 2019). Specifically, the higher RHP values (mainly due to uranium; Table 4) are related to shales of the Olmos Formation, located northeast of the study area (north of the Las Esperanza volcanic field) in areas with a high geothermal gradient and relatively high heat flow (62–67 mWm^{-2}) proposed by Carrillo-de la Cruz et al. (2020). The shales (also sandstones) of this formation belong to the coal seam carrier sequence, in which these rocks are characterized by high contents of transformed organic matter (Eguiluz de Antuñano 2001) and clay, quartz, and feldspar (Piedad-Sánchez et al. 2015), minerals that can contribute to the concentrations of radioelements (IAEA 2003). This mineral and organic matter content could be the principal cause of the high eU, eTh, and K concentrations and, therefore, the high RHP of these rocks (Vila et al. 2010). Moreover, other causes for the higher RHP may be related to the low thermal conductivities of the shales, which allow heat to remain inside these rocks over long geological timescales (McCay et al. 2014). The site of this Olmos Formation shales is located close to a deep geological structure (La Babia Fault) in a zone where Carrillo-de la Cruz et al. (2020) previously reported a relatively high heat flow (62–67 mWm^{-2}), obtained through Curie temperature depths estimated from aeromagnetic data. Therefore, their relationship with that geological structure can also contribute to radioactive concentrations and RHP, which, in turn, contributes to heat flow.

The sandstones of the Pátula Formation are the second group of rocks that contribute the most to the RHP, mainly due to their eTh and K concentrations (Table 4). Such concentrations must be related to the type of sandstone (arkose) and their quartz and K-feldspars contents and other minerals (clays, muscovite, biotite, apatite, and zircon) reported by Ocampo-Díaz (2013), Ocampo-Díaz et al. (2014) and Batista-Rodríguez et al. (2017b). In other regions worldwide, such as Nigeria, rocks with high contents of these minerals present high concentrations of both mentioned radioelements (Akingboye et al. 2021). Therefore, the high RHP in these rocks would have mainly been related to their high SiO_2 and F-feldspars concentrations (Hasterok and Webb 2017; Hasterok et al. 2018). The site of the Pátula Formation is located in the proximity of the San Marco fault (Fig. 1) within a zone of high heat flow (67–73 mWm^{-2}; Carrillo-de la Cruz et al. 2020). Its relationship with this deep structure also contributes to its RHP values, and these, in turn, contribute to the heat flow recorded in this region.

The RHP comparison of these sandstones and shales with others located in different regions of the world, such as the United States, Finland, Australia, Norway, and China (Vila et al. 2010; Hasterok et al. 2018; Zhu et al. 2018) suggests that these rocks, mainly the Olmos Formations shales and Pátula Formation sandstones are more enriched in the minerals as quartz, and feldspars. Similarly, some limestones have higher RHP than in other regions, which must have mainly been related to the clay and quartz contents, reported by Lucas et al. (2010), Torres de la Cruz et al. (2020), and Loucks et al. (2021) in Cupido, Buda, and Austin Formation of the Sabinas Basin. Also, it is likely that the relationship of some deeply faulted shale and sandstone sites (La Falla and San Marco) has contributed to the higher RHP values relative to other regions.

The differences in radioactive element concentrations and RHP values between the three volcanic fields must be related to the U-, Th-, and K-bearing minerals content of these rocks (IAEA 2003), as well as their enrichment in incompatible elements (Slagstad 2008), and their degree of alteration (Dostal et al. 1984). Therefore, the basalts of Las Coloradas could be more enriched in bearing minerals U, Th, and K (IAEA 2003) and/or in incompatible elements and/or have less degree of alteration. In this research, only are available petrographic or geochemical data available for basalts de Ocampo y Las Esperanzas. Both volcanic fields are reported apatite, and in Ocampo, K-feldspars are reported (Valdez-Moreno 2001; Valdez-Moreno et al. 2011). The first mineral is a carrier of U and Th, while the latter is carrier K (IAEA 2003). Therefore, the basalts of the Las Coloradas volcanic field can have higher contents of apatite and K-feldspars. The presence of K-feldspars in the Ocampo basalts explains their higher radioactivity and RHP, concerning the Las Esperanzas field. The geochemical data referring to the K_2O contents (up to 2% in Ocampo and up to 1.6% in Las Esperanzas; Valdez-Moreno 2001; Valdez-Moreno et al. 2011) also justify this approach. It is possible that the relationship of these volcanic fields with high and low blocks of the basement could be another factor in their differences in the RHP. For example, Las Coloradas (with higher RHP) and Ocampo (with intermediate RHP) are located at the high basement block zones (Las Coloradas in the Coahuila block and Ocampo in La Mula Island; Fig. 1). On the other hand, Las Esperanza, with a lower RHP, is located at the zone of blocks below the basement within the Sabinas Basin. Also, the RHP values are related to the heat flow calculated by Carrillo-de la Cruz et al. (2020). The two volcanic fields with the highest RHP (Las Coloradas and Ocampo) are located above zones of relatively high heat

flow (67–73 mWm^{-2}), while Las Esperanzas is related to zones of lower heat flow (62–67 mWm^{-2}). This evidence the contribution of the rocks of these two volcanic fields to the reported heat flows.

The highest values of the three radioelements and the RHP in Marcelinos intrusion, followed by Pánuco, Providencia and Colorado, suggest higher U-, Th-, and K-bearing minerals contents, and possibly also silica, in the rocks of the Marcelinos intrusion than those of the Pánuco, Providencia, and Colorado bodies. This research does not have petrographic or geochemical data either about Marcelinos intrusion, but the petrography studies in the other three intrusions reported radioelement-bearing minerals (Valdez-Reyes 2001; Fuentes-Guzmán 2016; Herrera-León 2019). The main K-bearing minerals are K-feldspars (microcline, orthoclase), hornblende, and biotite, while U- and Th-bearing minerals are sphene, zircon, and apatite. Therefore, in the Marcelinos intrusion, the granodiorite must have higher contents of some of those mentioned minerals. According to the geochemical data available in the Pánuco, Providencia, and Colorado intrusions (Valdez-Reyes 2002; Fuentes-Guzmán 2016; Herrera-León 2019), the highest Si_2O, K_2O, and Th contents are obtained in the Pánuco rocks (Si_2O up to 70%, K_2O up to 12.69% and Th up to 25.7 ppm), and the lowest in Colorado (Si_2O up to 65%, K_2O up to 4% and Th up to 8 ppm) or Providencia (Si_2O up to 62%, K_2O up to 4.59% and Th up to 21 ppm). Therefore, these data also justify the higher contents of radioelements and RHP in Pánuco, compared to Providencia and Colorado. Pánuco's location in a high basement block (Monclova Island; Fig. 1) also contributes to its RHP values. The likely higher silica content in the Marcelinos intrusion may in fact indicate a higher degree of magmatic differentiation in the Marcelinos igneous body relative to the other three intrusions (Batista-Rodríguez et al. 2020). The contents of radioelements, RHP values, and the geochemical data indicate that the Pánuco intrusion must present a lower degree of magmatic differentiation than Marcelinos, but at the same time greater than Colorado and Providencia. Therefore, of the intrusive igneous rocks analyzed, the Marcelinos body had the least basic composition, and the Providencia body the most basic one. The radioactive element concentrations and RHP values of the Pánuco, Colorado, and Providencia igneous bodies were like those of the rocks comprising the Las Esperanzas and Ocampo volcanic fields. This similarity indicates that it is probable that both groups of rocks in those sites have similar contents of radioelements-bearing minerals.

All the igneous and sedimentary rock sites studied were located at the characterized areas by a high geothermal gradient and relatively elevated heat flow, as proposed by Carrillo-de la Cruz et al. (2020). According to Carrillo-de la Cruz et al. (2020), the magnetic sources in these areas and, therefore, the basement of the basin, is located at a shallow depth. Eguiluz de Antuñano (2001) reports depths from 1.7 to 6 km, and Batista-Rodríguez et al. (2017a) from 1.5 to 7 km. Both investigations indicate basin areas with a basement less than 2 km deep. The relatively high RHP values in the studied rocks indicate their contribution to the geothermal gradient and relatively high heat flow, reported in previous research.

Conclusions

Using in situ gamma radiation measurements, radiogenic heat production in rocks from the Sabinas Basin was determined. The analysis of the RHP in the Sabinas Basin showed that the sampled rocks could be classified as having low (< 2 μWm^{-3}), moderate (2–4 μWm^{-3}), and high (> 4 μWm^{-3}) RHP potentials. Most sampled rocks showed low RHP values below 2 μWm^{-3}. Only a little over 14% of the measurements indicated moderate and high RHP potentials. This proportion was mainly associated with clastic rocks (shales and sandstones) and intrusive igneous rocks (granodiorites). The highest RHP values are obtained in a shale site of the Olmos Formation, followed by another sandstone site of the Pátula Formation. Apparently the quartz, K-feldspars, and clay contents in these rocks, and their proximity to two deep faults (La Babia and San Marcos) are the causes of the highest RHP values reported. The variations in the radioelement-bearing minerals content (K-feldspars, sphene, zircon, and apatite) cause differences between in the RHP of the granodiorites of the four intrusions (Marcelinos, Colorado, Providencia, and Pánuco). According to the RHP values, these minerals should be more enriched in the Marcelinos intrusion and less enriched in the Colorado and Providencia intrusion. Also, the difference in the RHP of the three volcanic fields (Las Esperanzas, Ocampo, and Las Coloradas) is associated with radioelement-bearing minerals, such as K-feldspars and apatite, and also to their relationship with some paleo-structures of the region (high and low basement block). The two volcanic fields with the highest RHP, Las Coloradas, and Ocampo, are located at the two high basement blocks, the Coahuila Block and La Mula Island, respectively. The Las Esperanza volcanic field is located above a zone of low basement block. The relationship of the RHP values with previously reported heat flow zones indicates the radiogenic contribution of the measured rocks to these heat flows, therefore, these RHP values may be used in future updates of the heat flow schemes heat of the Sabinas Basin.

Acknowledgements We thank the Autonomous University of Coahuila and particularly the Higher School of Engineering for their support with this research.

Author contributions All authors contributed equally to the work.

Data availability Not applicable.

Declarations

Conflict of interest The authors declare that there is no conflict of interest.

References

Abbady AGE, Al-Ghamdi AH (2018) Heat production rate from radioactive elements of granite rocks in north and southeastern Arabian Shield Kingdom of Saudi Arabia. J Radiat Res Appl Sci 11:281–290. https://doi.org/10.1016/j.jrras.2018.03.002

Adagunodo TA, Bayowa OG, Usikalu MR, Ojoawo AI (2019) Radiogenic heat production in the coastal plain sands of Ipokia, Dahomey Basin, Nigeria. MethodsX 6:1608–1616. https://doi.org/10.1016/j.mex.2019.07.006

Aisabokhae J, Tampul H (2020) Statistical variability of radiation exposures from Precambrian basement rocks, NW Nigeria: implication on radiogenic heat production. Sci Afr 10:e00577. https://doi.org/10.1016/j.sciaf.2020.e00577

Akingboye AS, Ogunyele AC, Jimoh AT, Adaramoye OB, Adeola AO, Ajayi T (2021) Radioactivity, radiogenic heat production and environmental radiation risk of the Basement Complex rocks of Akungba-Akoko, southwestern Nigeria: insights from in situ gamma-ray spectrometry. Environ Earth Sci 80:228. https://doi.org/10.1007/s12665-021-09516-7

Aranda-Gómez JJ, Luhr JF, Housh TB, Valdez-Moreno G, Chávez-Cabello G (2005) El volcanismo tipo intraplaca del Cenozoico tardío en el centro y norte de México: una revisión. Bol Soc Geol Mex 57(3):187–225. https://doi.org/10.18268/bsgm2005v57n3a1

Barboza-Luna D, Martínez-Ramos CJ, Santiago-Carrasco B, Izaguirre-Ramos MA, Gracia-Valadez MJ (2008) Carta geológico-minera Tlahualilo de Zaragoza, G13-6, Coahuila, Durango y Chihuahua, 1:250,000. Servicio Geológico Mexicano. 1 mapa

Batista-Rodríguez JA, Almaguer-Carmenates Y, Martínez-González JD (2017a) Interpretation of aeromagnetic data using GIS to evaluate the geotectonic regime of the Sabinas Basin. Earth Sci Res J 21(4):175–181. https://doi.org/10.15446/esrj.v21n4.57924

Batista-Rodríguez JA, Proenza-Fernández JA, Rodríguez-Vega A, López-Saucedo F, Cázares-Carreón KI (2017b) Magnetic susceptibility and natural gamma radioactivity as indirect proxies for characterization of sandstones and limestones of Sabinas Basin. Geofizika 34(1):19–43. https://doi.org/10.15233/gfz.2017.34.6

Batista-Rodríguez JA, Niño-Rodríguez E, Rodríguez-Riojas PA, Díaz-Martínez R, Rodríguez-Vega A, López-Saucedo F (2020) In situ magnetic susceptibility and gamma radiation data in the Candela-Monclova intrusive belt, Northeast Mexico: case studies of the Cerro Colorado and Cerro Marcelinos pluton. Turk J Earth Sci 29:579–595. https://doi.org/10.3906/yer-1905-21

Carrillo-de la Cruz JL, Prol-Ledesma RM, Gómez-Rodríguez D, Rodríguez-Díaz AA (2020) Analysis of the relation between bottom hole temperature data and Curie temperature depth to calculate geothermal gradient and heat flow in Coahuila, Mexico. Tectonophysics 780:228397. https://doi.org/10.1016/j.tecto.2020.228397

Carrillo-de la Cruz JL, Prol-Ledesma RM, Gabriel G (2021) Geostatistical mapping of the depth to the bottom of magnetic sources and heat flow estimations in Mexico. Geothermics 97:102225. https://doi.org/10.1016/j.geothermics.2021.102225

Chávez-Cabello G, Aranda-Gómez JJ, Molina-Garza RS, Cossío-Torres T, Arvizu-Gutiérrez IR, González-Naranjo GA (2005) La falla San Marcos: una estructura jurásica de basamento Multirreactivada del noreste de México. Bol Soc Geol Mex 57:27–52. https://doi.org/10.18268/bsgm2005v57n1a2

Cui Y, Zhu C, Qiu N, Tang B, Guo S (2019) Radioactive heat production and terrestrial heat flow in the Xiong'an area, North China. Energies 12(24):4608. https://doi.org/10.3390/en12244608

Dostal J, Dupuy C, Chikhauoi M, Zentilli M (1984) Uranium and thorium in Late Proterozoic volcanic rocks from northwestern Africa. Chem Geol 42:297–306

Eguiluz de Antuñano S (2001) Geologic evolution and gas resources of the Sabinas Basin in Northeastern Mexico. In: Bartolini C, Buffler, RT, Cantú-Chapa A (eds) The western Gulf of Mexico Basin: tectonics, sedimentary basins, and petroleum systems, 75. AAPG Mem, pp 241–270. https://doi.org/10.1306/M75768C10.

Fuentes-Guzmán EF (2016) Metalogenia de la mina de Pánuco, Coahuila, México. Master's Thesis, National Autonomous University of Mexico

González-Ramos A, Martínez-Ramos C, Izaguirre-Ramos MA, Barboza-Luna D, Santiago-Carrasco B (2008) Carta geológico-minera Monclova, G14-4, Coahuila y Nuevo León, 1:250,000. Servicio Geológico Mexicano. 1 mapa.

Hasterok D, Webb J (2017) On the radiogenic heat production of igneous rocks. Geosci Front 8(5):919–940. https://doi.org/10.1016/j.gsf.2017.03.006

Hasterok D, Gard M, Webb J (2018) On the radiogenic heat production of metamorphic, igneous, and sedimentary rocks. Geosci Front 9:1777–1794. https://doi.org/10.1016/j.gsf.2017.10.012

Herrera-León MA (2019) Petrografía y geoquímica del intrusivo Colorado, Cinturón Candela-Monclova, provincial alcalina oriental mexicana. Bachelor's Thesis, Autonomous University of Nuevo León, México

Iglesias ER, Torres RJ, Martínez-Estrellas JI, Reyes-Picasso N (2015) Summary of the 2014 assessment of medium-to-low temperature Mexican geothermal resources. Proceedings World Geothermal Congress 2015, Melbourne, Australia, 10–25. https://pangea.stanford.edu/ERE/db/WGC/papers/WGC/2015/16081.pdf. Accessed April 2015

International Atomic Energy Agency, IAEA (2003) Guidelines for Radioelement Mapping Using Gamma Ray Spectrometry Data, IAEA-TECDOC-1363, IAEA, Vienna, Austria. https://www-pub.iaea.org/mtcd/publications/pdf/te_1363_web.pdf, Accessed 23 Feb 2021. Accessed 01 Nov 2022

Loucks RG, Reed RM, Ko LT, Zahm CK, Larson TE (2021) Micropetrographic characterization of a siliciclastic-rich chalk; Upper Cretaceous Austin Chalk Group along the onshore northern Gulf of Mexico, USA. Sediment Geol 412:105821. https://doi.org/10.1016/j.sedgeo.2020.105821

Lucas SG, Krainer K, Spielmann JA, Durney K (2010) Cretaceous stratigraphy, paleontology, petrography, depositional environments, and cycle stratigraphy at Cerro de Cristo Rey, Doña Ana County, New Mexico. N M Geol 32(4):103–130

Martínez-Estrella I, Torres RJ, Iglesias ER (2005) A GIS-Bases Information System for Moderate-to-Low-Temperature Mexican Geothermal Resources. Proceedings World Geothermal Congress 2005, Antalya, Turkey, 24–29. https://www.geothermal-energy.org/pdf/IGAstandard/WGC/2005/1725.pdf. Accessed Apr 2005

Martínez-Rodríguez L, Miranda A, Pérez MA, Romero I, Sánchez E (2008) Carta geológico-minera Nueva Rosita, G14-1, Coahuila y Nuevo León, 1: 250 000. Servicio Geológico Mexicano. 1 mapa

McCay AT, Harley TL, Younger PL, Sanderson DCW, Cresswell AJ (2014) Gamma-ray spectrometry in geothermal exploration: state of the art techniques. Energies 7:4757–4780. https://doi.org/10.3390/en7084757

Nagihara S, Sclater J, Phillips J, Behrens E, Lewis T, Lawver L, Nakamura Y, Garcia-Abdeslem J, Maxwell A (1996) Heat flow in the western abyssal plain of the Gulf of Mexico: implications for thermal evolution of the old oceanic lithosphere. J Geophys Res Solid Earth 101(B2):2895–2913. https://doi.org/10.1029/95JB03450

Netto A (2017) Delineating the ocean-continent crustal boundary in the Gulf of Mexico using Heat Flow Measurements. Master's Thesis, Texas Tech University, US. https://ttu-ir.tdl.org/bitstream/handle/2346/73140/NETTO-THESIS-2017.pdf?sequence=1

Ocampo-Díaz YZE (2013) Análisis petrográfico y estadístico multivariado para discriminar las áreas fuente de la Formación La Casita del Jurásico Tardío-Cretácico Temprano y la Arcosa Patula del Cretácico Temprano en el Noreste de México. Bol Soc Geol Mex 65(3):609–630

Ocampo-Díaz YZE, Talavera-Mendoza O, Jenchen U, Valencia VA, Medina-Ferrusquia HC, Guerrero-Suastegui M (2014) Procedencia de la Formación La Casita y la Arcosa Patula: implicaciones para la evolución tectono-magmática del NE de México entre el Carbonífero y el Jurásico. Rev Mex Cienc Geol 31(1):45–63

Padilla y Sánchez RJ (1986) Post-Paleozoic tectonics of Northeast Mexico and its role in the evolution of the Gulf of Mexico. Geofis Int 25:157–206

Pérez-De la Cruz JA, De los Santos-Montaño J, Arzabala-Molina J, Tarín-Zapata G (2008) Carta geológico-minera Ocampo, G13-3, Coahuila y Chihuahua, 1:250,000. Servicio Geológico Mexicano. 1 mapa

Piedad-Sánchez N., González-Partida E, Vega-González M, De la Rosa-Rodríguez G, Garza-Blackaller S, Muñoz-García JL, Corona-Esquivel R (2015) Madurez térmica del carbón en un área de Las Esperanzas, Coah., Municipio de Melchor Múzquiz, Coah. XXI Convención Internacional de Minería, Acapulco, Guerrero, México. 127–132. https://www.geomin.com.mx/publicaciones/pub4_XXXI%20Conv_AIMMGM%20Memorias.pdf. Accessed Sept 2023

Prol-Ledesma RM, Morán-Zenteno DJ (2019) Heat flow and geothermal provinces in Mexico. Geothermics 78:183–200. https://doi.org/10.1016/j.geothermics.2018.12.009

Prol-Ledesma RM, Carrillo-de la Cruz JL, Torres-Vera MA, Membrillo-Abad AS, Espinoza-Ojeda OM (2018) Heat flow map and geothermal resources in Mexico. Terra Digit 2(2):1–15. https://doi.org/10.22201/igg.25940694.2018.2.51.105

Romo-Ramírez JR, Herrera-Monreal JC, Rodríguez-Rodríguez JS, Larrañaga-Obregón G (2008) Carta geológico-minera San Miguel, H13-12, Coahuila y Chihuahua, 1:250 000. Servicio Geológico Mexicano. 1 mapa.

Radiation Solution Inc. (2015) RS-125/230 User Manual. Revision 1.05—December 2015. https://www.aseg.org.au/sites/default/files/RS-125%20RS-230_User_Manual%20%28GR%29.pdf. Accessed 01 Nov 2022.

Rybach L (1988) Determination of heat production rate. In: Hänel R, Rybach L, Stegena I (eds) Handbook of terrestrial heat-flow density determination. Kluwer academic Publishers, Amsterdam, pp 125–142

Santiago-Carrasco B, Ontiveros-Escobedo E, Martínez-Rodríguez L, Herrera-Monreal JC (2008) Carta geológico-minera Piedras Negras, H14-10, Coahuila, 1:250,000. Servicio Geológico Mexicano. 1 mapa

Slagstad T (2008) Radiogenic heat production of Archean to Permian geological provinces in Norway. Norw J Geol 88:149–166

Tolentino-Álvarez J (2022) Caracterización geológica, geofísica y geoquímica de manifestaciones geotérmicas del estado de Coahuila. Master's Thesis, Autonomous University of Coahuila, Mexico

Torres de la Cruz FJ, Chacón-Baca E, Chávez-Cabello G, Hernández-Ocaña MI (2020) Revisiting the Cupidito unit (Cupido Formation) along peritidal carbonates from northeastern Mexico. Rev Mex Cienc Geol 37(1):9–25. https://doi.org/10.22201/CGEO.20072902E.2020.1.1095

Torres-Rodríguez V, Arellano-Gómez V, Barragán-Reyes RM, González-Partida E, Herrera-Franco JJ, Santoyo-Gutiérrez E, Venegas-Salgado S (1993) Geotermia en México. Programa Universitario de Energía, Universidad Nacional Autónoma de México

Valdez-Moreno G (2001) Geoquímica y petrología de las rocas ígneas de los campos volcánicos Las Esperanzas y Ocampo, Coahuila, México. Master's Thesis, National Autonomous University of Mexico

Valdez-Moreno G, Aranda-Gómez JJ, Ortega-Rivera A (2011) Geoquímica y petrología del campo volcánico de Ocampo, Coahuila, México. Bol Soc Geol Mex 63(2):235–252

Valdez-Reyes MA (2001) Petrografía y geoquímica del intrusivo Cerro Providencia, margen este del Cinturón Candela-Monclova, provincial alcalina oriental mexicana. Master's Thesis, Autonomous University of Nuevo León, México

Vila M, Fernández M, Jiménez-Munt I (2010) Radiogenic heat production variability of some common lithological groups and its significance to lithospheric thermal modeling. Tectonophysics 490:152–164. https://doi.org/10.1016/2Fj.tecto.2010.05.003

Wilson JL (1990) Basement structural controls on Mesozoic carbonates facies in northeastern Mexico: a review. In: Tucker ME, Wilson JL, Crevello PD, Sarg JR, Read JF (eds.), Carbonate platforms, facies, sequences and evolution, vol 9. IAS, pp 235–255

Wolaver BD, Crossey LJ, Karlstrom KE, Banner JL, Cardenas MB, Gutiérrez-Ojeda C, Sharp JM Jr (2013) Identifying origins of and pathways for spring waters in a semiarid basin using He, Sr, and C isotopes: Cuatrociénegas Basin, Mexico. Geosphere 9(1):113–125. https://doi.org/10.1130/GES00849.1

Zhu Ch, Xu M, Qiu N, Hu S (2018) Heat production of sedimentary rocks in the Sichuan basin, Southwest China. Geochem J 52(5):401–413. https://doi.org/10.2343/geochemj.2.0530